ELSEVIER

Journal of Power Sources 106 (2002) 126–135

JOURNAL OF POWER SOURCES

www.elsevier.com/locate/jpowsour

Investigation of the degradation of different nickel anode types for alkaline fuel cells (AFCs)

E. Gülzow, M. Schulze*, G. Steinhilber

Institut für Technische Thermodynamik, Deutsches Zentrum für Luft- und Raumfahrt, Pfaffenwaldring 38-40, D-70569 Stuttgart, Germany

Abstract

Alkaline fuel cells (AFCs) have the opportunity of becoming important for mobile energy systems as, in contrast to other low temperature fuel cells, the alkaline type requires neither noble metal catalysts nor an expensive polymer electrolyte.

In AFCs, nickel is used as anode catalyst in gas diffusion electrodes. The metal catalyst was mixed with polytetraflourethylene (PTFE) as organic binder in a knife mile and rolled onto a metal web in a calendar to prepare the electrode. After an activation process with hydrogen evolution at 5 mA/cm^2 for 18 h, the electrodes were stressed at constant loading in a half cell equipment. During the fuel cell operation, the electrochemical performance decreased due to changes of the polymer (PTFE) and of the metal particles in the electrode, which is described in detail in another paper.

In this study, three types of electrodes were investigated. The first type of electrode is composed of pure Raney-nickel and PTFE powder, the nickel particles in the second electrode type were selected according to particle size and in the third electrode copper powder was added to the nickel powder not selected by size. The size selected nickel particles show a better electrochemical performance related to the non-selected catalyst, but due to the electrochemically induced disintegration of the nickel particles the electrochemical performance decreases stronger. The copper powder in the third electrode is added to improve the electronic conductivity of the nickel catalyst, but the copper is not stable under the electrochemical conditions in fuel cell operation. With all three anode types long-term experiments have been performed. The electrodes have been characterized after the electrochemical stressing to investigate the degradation processes.

Keywords: Alkaline fuel cell; Anodes; Nickel particles; Degradation; Characterization of electrodes

1. Introduction

Much attention has been paid to fuel cells because they offer a highly efficient and environmentally friendly technology for energy conversion avoiding the Carnot limitations of combustion engines. Low temperature fuel cells as polymer membrane fuel cells (PEFC) and direct methanol fuel cells (DMFC) as well as alkaline fuel cells (AFCs) are considered as a most promising option for powering future cars [1,2] and small combined power units due to their modular construction and the high energy densities that can be attained.

Each type of the low temperature fuel cells has individual advantages compared to the other types. One advantage of AFC is that no expensive noble metal is necessary as catalyst, due to lower corrositivity of a basic environment compared to an acid one. Nickel can be used as catalyst in the anode and silver in the cathode. A second advantage is that the liquid electrolyte can be used for the regulation of the temperature in the fuel cell.

In addition to the costs of fuel cells, the lifetime of fuel cells is a general problem for the technical utilization in stationary or mobile applications. During lifetime, the fuel cell performance and the fuel cell behavior should not change significantly. The end of the lifetime is induced by changes of fuel cell components, which results at last in a decrease of the electrochemical performance. To understand the decrease in the electrochemical performance, the knowledge about the changes of the fuel cell components and their causes as well as the understanding of the influence of the changes of the individual components to the fuel cell operation are necessary. Therefore, studying the changes of single fuel cell components is the first step to investigate the degradation of fuel cells. Numerous papers have investigated the degradation of solid oxide fuel cell components—anodes [4–10], cathodes [11–19], electrolyte [20–23], interconnectors [24–26], etc. For PEFC, some studies are published which have investigated the degradation of bipolar plates [27,28], the electrolyte membrane [29–32] or the catalyst [33–36] and the electrochemical performance [3,37,38]. The

* Corresponding author. Tel.: +49-711-6862-456; fax: +49-711-6862-747.
E-mail address: mathias.schulze@dlr.de (M. Schulze).

0378-7753/02/$ – see front matter
PII: S0378-7753(01)01033-3

AFC can be separated without any problem into the components, which allows to investigate the components with a lot of different methods. This gives a significant advantage for the study of degradation processes, but only few studies on the electrochemically induced changes of AFC components exist [39–46].

The investigated anodes consist of a metallic catalyst, PTFE and possibly with additives on a metal web. The catalyst is necessary for the electrochemical reaction and the electrical conduction to the metal web. The metal web serves as stable carrier for the electrode and for the electric conduction. The PTFE is hydrophobic and, thus, prevents the electrode from being totally flooded by the electrolyte which penetrates into the pore system. It also allows the gas transport in the electrode; consequently, the three phase zone where the electrochemical reaction takes place is not only on the electrode surface, but also formed in the volume of the electrodes. In addition, the PTFE works as organic binder fixing the catalyst particles in the electrode.

At DLR low temperature fuel cells are investigated focussing on the preparation of gas diffusion electrodes and membrane–electrode assemblies, electrochemical behavior, physical characterization, long-term behavior and degradation mechanisms. The preparation of the gas diffusion electrode based on Sauer [47] and Winsel [48] has been further developed for electrodes of different low-temperature fuel cell types, AFC [49–55] and PEFC [33,56–59] as well as for other electrochemical applications [60].

In this paper, the degradation of three different electrode types has been investigated: type 1 electrodes consist of an mixture of pure Raney-nickel and PTFE powder onto an nickel web, type 2 electrodes consist of an mixture of a Raney-nickel catalyst with an addition of copper powder and PTFE powder onto a copper web, for the electrodes of type 3 the nickel catalysts were size-selected before electrode preparation. The nickel catalyst is a highly porous metallic catalyst which is formed from an aluminum–nickel alloy by dissolving the aluminum. The used basic alloy for the catalyst and the PTFE powder is the same in all electrodes.

The electrodes of type 2 were investigated in an earlier study, which will be described in detail in a paper to be published in future [61]. The different changes of nickel electrodes are observed after electrochemical operation as AFC anodes. During operation time a decrease of the electrochemical performance was observed [43,46]. The physical characterization of the electrodes after operation shows that the pore size distribution has changed [46], whereby the specific surface is nearly unchanged. The nickel catalyst particles are disintegrated during electrochemical operation. If the anodes are overloaded, so that the polarization of the electrodes is high, the nickel will be oxidized [43]. The copper is partially dissolved in the electrolyte. Residual aluminum contains will be further dissolved during fuel cell operation [43]. The PTFE is changed by the electrochemical loading [42]. This result is very surprising because PTFE should be stable in all electrochemical environments. In addition, PTFE is also used in PEFC, which are at present a main topic of the fuel cell research.

The same changes are also observed during the activation process of the electrodes [45] as well as a dissolving of the copper, whereby the copper is transported through the surface to the electrolyte. In X-ray photoelectron spectroscopy measurements a change of the copper concentration on the electrode surface, which depends on time and current density (i), was observed.

2. Experimental

2.1. Electrode preparation

Three types of electrodes were investigated. The electrodes were prepared in the same way from a porous nickel catalyst and PTFE powder. The porous nickel catalyst used consisted of a nickel–aluminum alloy containing 50 wt.% of each metal. In a KOH, the catalyst was activated by dissolving the aluminum at 350 K. After this procedure, the catalyst contained less than 5% of aluminum. During the activation process, the nickel was loaded with 0.5–1.2 hydrogen atoms per nickel atom [62]. After this preparation of the catalyst, the powder was washed and dried. Due to the hydrogen in the metal and the reactivity of a metallic nickel surface contact with oxygen during the drying process has to be avoided. The catalyst powder cannot be handled in the reactive state to produce the electrodes. Therefore, after drying the catalyst powder was passivated by controlled oxygen exposure under temperature control of the powder. During this preparation step, the hydrogen was removed and the catalyst surface was oxidized.

The passive catalyst and PTFE powder were mixed in a knife mile, rolled to a strip and fixed onto a metal web. To enhance the electrical conductivity in the electrode, metallic copper powder was added to the mixture of the nickel catalyst and PTFE.

The type 1 electrodes were prepared from the nickel catalyst and PTFE powder without any additives. As metallic web for the electrical conduction nickel was used. In the electrodes of type 2 copper was added to the powder mixture and a copper web was used for the electrical conduction. The nickel particles which are used in the type 3 electrodes were size selected, so that large particles were separated from the catalyst powder, before the powders were mixed in the knife mile. Like the type 2 electrodes a copper web was also used for the type 3 electrodes.

Due to the passivation of the nickel catalyst the electrodes must be activated before being used in the electrochemical devices. The electrodes were activated in a standard procedure by hydrogen developing at 5 mA/cm^2 for 18 h in a 30% KOH [45]. During this activation procedure the oxidized nickel was reduced to metallic nickel, the copper was partially dissolved, the specific surface area increased and the pore size distribution changed [45].

2.2. Electrochemical operation conditions and characterization

The electrodes were activated in an electrochemical half cell configuration consisting of the electrode in a holder manufactured from Plexiglas, a nickel counter electrode and a Hg/HgO reference electrode. In the experimental setup, the electrodes were supplied with pure hydrogen without overpressure from the backside with the metallic web. The electrode holder was inserted into a tempered vessel containing 30% KOH. The same setup was used for the electrochemical characterization of fuel cell electrodes. The electrode has an active area of 6 cm^2.

After activation the electrodes were electrochemically loaded with a constant current density; the electrodes operated at 353 K. For most of the experiments, the electrodes were stressed with a current density of 100 mA/cm^2. For the electrochemical characterization, *V–i* curves were recorded. For this purpose, the current density was set in increasing steps and the electrode potential was recorded after the potential had become stable. The influence of the Ohmic losses in the measured potential was corrected by *I–R* drop measurements; the current was disconnected with a fast electronic switch and any resulting change of the potential was recorded by a digital oscilloscope. The initial potential step gives the voltage decrease over the Ohmic resistance from the conducting of the electrode and in the electrolyte; it is used for correcting the potential. The following exponential change of the electrode potential is the consequence of the electrochemical polarization.

To study the influence of overloading the electrodes were damaged by stressing with high current densities up to 400 mA/cm^2, whereby the electrode polarization reached the potential range where nickel oxide can be formed. The electrodes were damaged by decreasing the KOH concentration significantly.

To describe the long-term behavior of the electrochemical performance we defined a parameter called surface specific conductivity. For low current densities, the *V–i* curve has nearly a linear run, so we defined the gradient of the *V–i* curve as surface specifical conductivity. The current density divided by the polarization at 100 mV overvoltage gives nearly the same value. In this definition, a high surface specifical conductivity means a high electrochemical performance and a decrease is related to a decrease of the electrochemical performance. Fig. 1 shows a typical *V–i* curve. The reciprocal gradient of the added straight line is the surface specifical conductivity.

2.3. Physical characterization of the electrodes after electrochemical operation

The electrodes were removed from the test setup to perform the surface analysis and rinsed with distilled water after being removed from the half cell configuration. Subsequently, the electrodes were separated to different samples for the different applied characterization methods and individually dried under the conditions required for the different analyzing methods. For each measurement, a new electrode was used. The electrodes were characterized by X-ray photoelectron spectroscopy (XPS) to analyze the chemical composition of the surface [63], scanning electron microscopy (SEM) with energy dispersive X-ray spectroscopy (EDX) [63] to determine the structure and element distribution and nitrogen adsorption [64] to investigate the pore size distribution.

The investigated GDE and the different parts were dried before being analyzed under typical conditions.

The XPS characterization of the electrodes was performed in a standard UHV chamber equipped with an XP-spectrometer (spherical analyzer $r = 127$ mm, 300 W X-ray tube with Al- and Mg-excitation) and a quadrupole

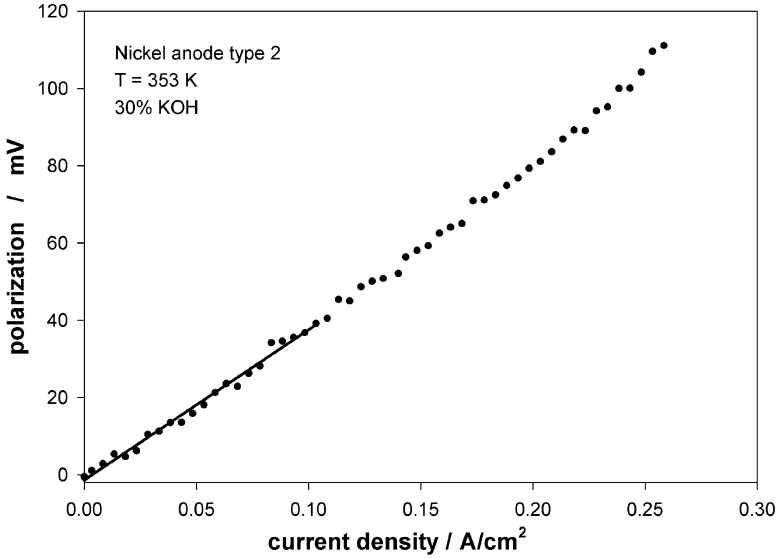

Fig. 1. Typical *V–i* curve. From the shown straight line, the surface specifically conductivity will be calculated.

mass spectrometer. The residual pressure in the analysis chamber was approximately $P \approx 4 \times 10^{-10}$ mbar. The composition of the residual pressure gas was verified by the mass spectrometer. After being rinsed with distilled water the electrodes were subsequently dried in the vacuum lock at 350 K for 8 h. The pressure increased by nearly two orders of magnitude after transferring the GDE sample into the UHV chamber. To investigate the GDE, XP spectra of the C 1s, F 1s, Ni 2p, Cu 2p and O 1s levels were recorded during depth profiling by alternating XPS measurements and ion etching. During depth profiling of GDEs, the etching period was increased after 10 cycles. The changes of the surface composition during the depth profiling are not only induced by the etching of the surface, but also by the decomposition of the polymer induced by the ionizing irradiation [42]. The experimental conditions, drying temperature and time, X-ray doses and Ar^+ ion doses during the ion etching, were kept constant for all samples.

For the SEM/EDX measurements a TOPCON DS130 microscope and a NORAN VOYAGER 3000 EDX-system were used. The microscope beam energy can be varied in the range of 1–40 keV, the maximum resolution of the SEM is 3 nm. The EDX analyzer is equipped with an ultra-thin window, allowing light element analysis from carbon upwards. The electrode samples were dried in air after being washed in distilled water before starting the SEM and EDX analyses.

The porosimetry and the specific surface were measured by adsorption of nitrogen [65]. For these measurements, the samples were dried in vacuum at 400 K for 18 h. The nitrogen adsorption measurements were performed in a commercial system (Carlo Erba Sorptomatic Series 1800) and were evaluated with the standard BET algorithms [64].

3. Results and discussion

The electrodes of types 1 and 2 have nearly the same initial electrochemical performance after their activation. The initial performance of the electrodes of type 3 is slightly improved. The same initial electrochemical performance of the types 1 and 2 electrodes results from the identical nickel catalyst in both electrodes. The improvement of the electrical conductivity by the copper does not results in a better electrochemical performance. In contrast, the size-selected nickel catalyst in the electrode of type 3 leads to an improved electrochemical performance. In the electrochemical long-term experiments, a decrease of the performance is observed for all the three electrode types as shown in Fig. 2. The decrease of the electrochemical performance (Perf) is not linear for each investigated electrode and it can be approximated with a function of the following type:

$$\mathrm{Perf}_1(t) = a \exp\left\{-\frac{t}{t_0}\right\} + c. \quad (1)$$

If the polarization during the electrochemical loading increases significantly over 100 mV induced by the decreasing electrochemical performance, the electrode rapidly loses its electrochemical performance as shown for the lifetime curve of the electrode of type 1 at on operation time of 1200 h.

For the electrodes of types 2 and 3, long-term experiments with different electrochemical loadings were performed; with the type 1 electrode long-term tests with different electrochemical loadings were not performed. The initial electrochemical performance of different samples of one electrode type differs by a maximum 20%, which can be explained by different electrochemical active areas after the activation procedure. Electrodes of type 2 were loaded with a current density from 25 up to 300 mA/cm^2, whereby long-term tests

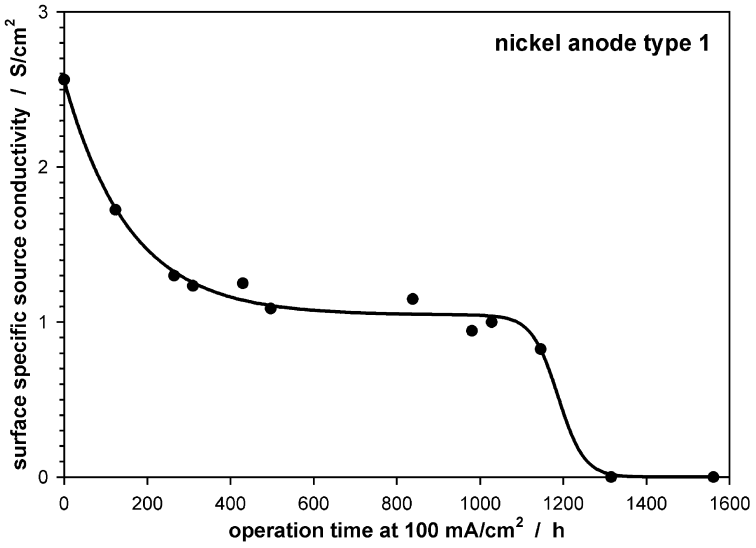

Fig. 2. Time-dependent surface specific source conductivity of a nickel anode of type 1 recorded at a current density of 100 mA/cm^2.

were performed at 50, 100, 150 and 200 mA/cm^2. Fig. 2 shows the time curve of the electrochemical performance of a type 1 electrode. Electrodes of the type 3 were loaded at 100 and 150 mA/cm^2 in long-term experiments. Fig. 3 shows the decrease of the electrochemical performance of type 2 electrodes operating at different current densities. In Fig. 3c, the time curves of the electrochemical performance have been normalized by the different initial electrochemical performance to compare the different samples. The decrease of the electrochemical performance of type 3

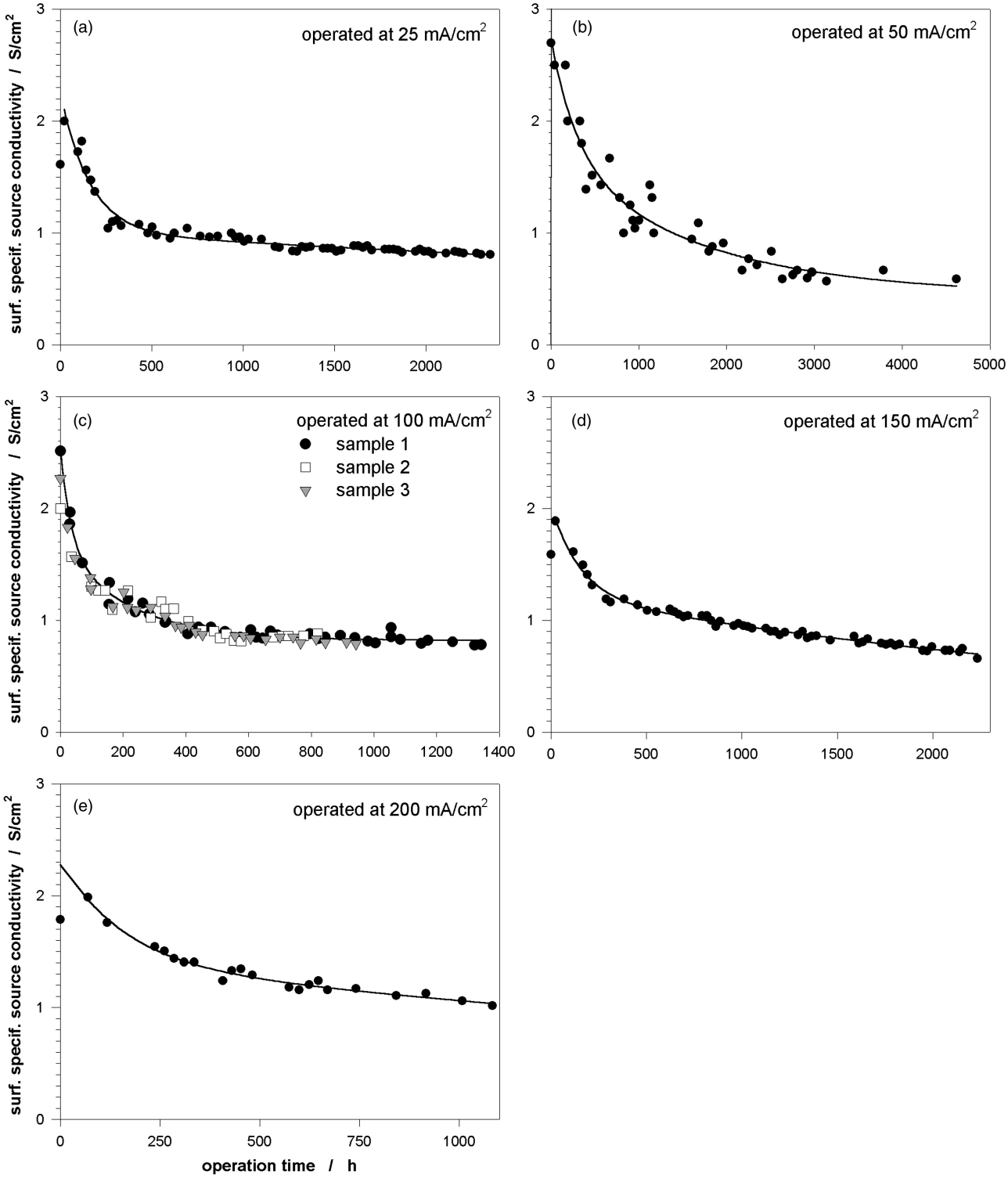

Fig. 3. Time-dependent surface specific source conductivity of a nickel anode of type 2 recorded at a different current density: (a) 25 mA/cm^2; (b) 50 mA/cm^2; (c) 100 mA/cm^2; (d) 150 mA/cm^2; and (e) 200 mA/cm^2.

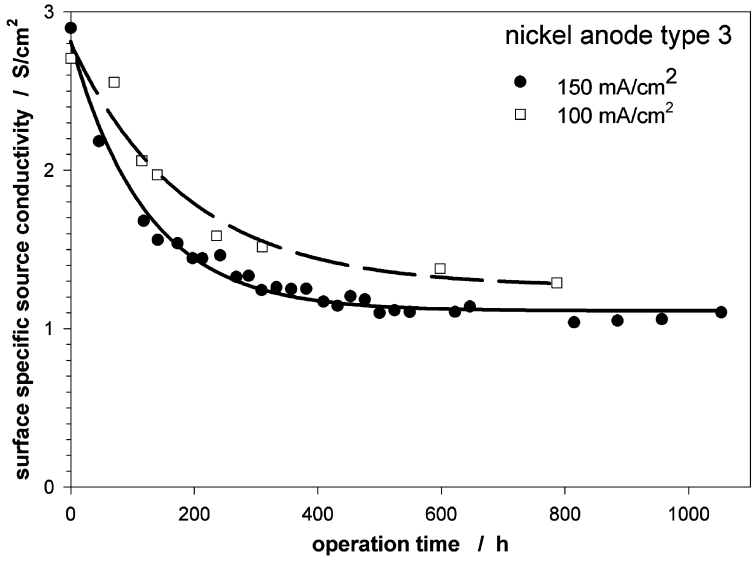

Fig. 4. Time-dependent surface specific source conductivity of a nickel anode of type 3 recorded at a different current density: dashed line, 100 mA/cm^2; solid line, 150 mA/cm^2.

electrodes operating at different current densities is given in Fig. 4.

The decrease of the electrochemical performance of type 2 electrodes cannot described with an single exponential function of the type 1. The time dependent electrochemical performance can be described by the combination of two e-function in form of following form:

$$\mathrm{Perf}_2(t) = a\exp\left\{-\frac{t}{t_0}\right\} + b\exp\left\{-\frac{1}{t_1(i)}\right\} + c \qquad (2)$$

The first e-function only depends on the time, the second e-function on current density (i) and time (t).

In contrast for the electrodes of type 3, the time-dependent electrochemical performance can be described with a single e-function, whereby the e-function depends on the charging density.

$$\mathrm{Perf}_3(t) = a\exp\left\{-\frac{t}{t_0(i)}\right\} + c \qquad (3)$$

The decrease of the electrochemical performance of the three electrode types is not very different. For the electrodes of types 1 and 3 at the described operation conditions and a current density of 100 mA/cm^2, a time constant t_0 of approximately 250 h was determined from the long-term behavior of the surface specifical source conductivity using Eq. (1) and (3). For the electrodes of type 2 at 100 mA/cm^2 for one term of Eq. (2) one of the two time constants (t_0) was also determined to be approximately 250 h. The time constants for all electrode types are nearly the same.

At higher current densities for the type 3 electrode the time constant for the decrease of the surface specific source conductivity at 150 mA/cm^2 was determined to approximately 100 h. This indicates that the decrease of the electrochemical performance does not depend on the electrochemical loading alone. At higher current densities, the degradation is accelerated more than the ratio of the current densities. For the electrode of type 2, this time constant does not depend on the current density so strongly; it ranged from approximately 300 h at 50 mA/cm^2 up to 150 h at 200 mA/cm^2. The time constant of the second term in Eq. (2) which is necessary depends much more on the current density, indicating that two different degradation processes are relevant for the type 2 electrodes.

The disintegration of the nickel particles should be comparable for the electrodes of types 1 and 2, because the same catalyst is used in both electrodes. Due to the size-selection of the nickel catalyst in the type 3 electrodes, the consequence of the nickel particles disintegration differs from that of the other electrodes. For all electrode types, the concentration of small nickel particles increases, but because of the disintegration of large nickel particles in electrodes of types 1 and 2, nickel particles of different sizes are rebuilt so that the change of the size distribution is not so significant as for the nickel catalyst in type 3 electrodes; only the large nickel catalyst particles are removed from the particle size distribution in types 1 and 2 electrodes. In the electrodes of type 3, the initial particle size distribution is shifted to lower particle sizes.

As a consequence of the disintegration of the nickel catalysts the pore size distribution determined by nitrogen adsorption measurements changes. The pore size distributions of electrodes of types 2 and 3 were recorded after different operation times, whereby for each measurement one electrode was necessary. The nitrogen adsorption measurements show that the pore size distribution is dominated by pores with a pore radius of 2 nm, which is related to the pore system of the Raney-nickel catalyst [45]. Fig. 5 shows the pore frequency at 2 nm pore radius for the electrodes of types 2 and 3 as function of the operation time. For the type 2 electrodes, the pore frequency at 2 nm pore radius increases

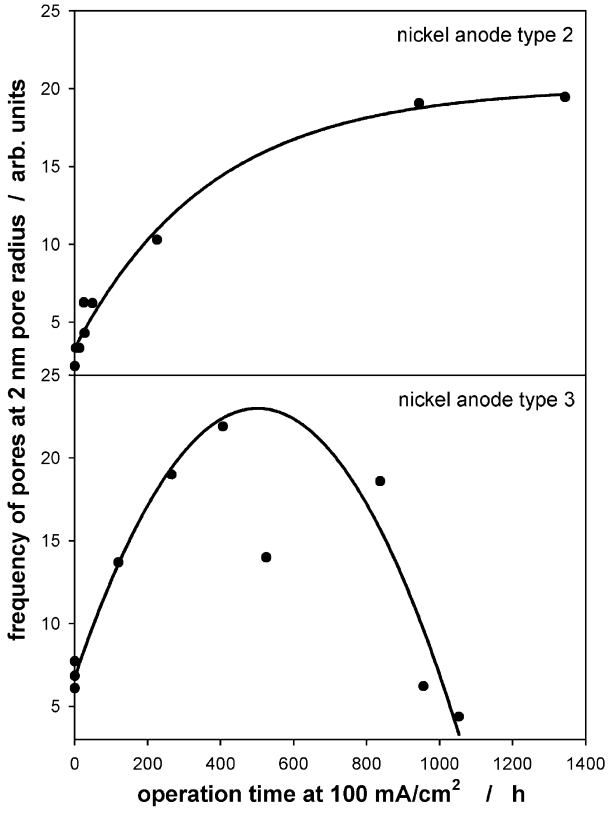

Fig. 5. Pore frequency at 2 nm as function of time recorded with nitrogen adsorption measurements of electrodes of type 2 (on the top) and type 3 (on the bottom). In the diagram, for the electrode of type 3, the data of four electrode samples, which were overloaded are added and marked with squares symbols.

during operation time. In contrast, for the electrodes of type 3 the pore frequency has a maximum at approximately 500 h operation time due to the size-selection of the nickel particles. For the type 2 electrode, a strong correlation between the pore frequency at 2 nm and the area specific source conductivity was observed [61], while such a correlation does not exist for the electrode of the type 3. During the disintegration of very small nickel particles, the pore system of the Raney-nickel disappeared and so the pore frequency at 2 nm decreased.

In addition to the pore size distribution, the specific surface area was recorded by the nitrogen adsorption measurement. Due to the disintegration of the nickel particles, it can be expected that the specific surface increases, but an increase of the specific surface was not observed. The specific surface area of the electrodes of type 2 decreased only slightly during operation time, in contrast the specific surface area of type 3 electrodes decreased by approximately 40% after an operation time of 1000 h.

The oxidation stability of the nickel catalyst is independent of the catalyst type, it only depends on the electrochemical potential. Therefore, for all electrode types, the nickel catalyst is oxidized, if the anodic polarization is too high. Therefore, the stability of the electrodes against overloading to high anodic potentials is the same for all electrode types. The electrodes which were overloaded for some time lost their electrochemical activity and the nickel catalyst was partially oxidized. The different oxidation states of the nickel can be distinguished in the XP spectra as shown in Fig. 6 [66,67]. A significant difference in the spectrum of metallic nickel and oxidized nickel can be seen in the satellite peaks of the nickel oxide. The active electrodes show metallic nickel like freshly activated electrodes. In the electrodes of type 3 the part of nickel oxide increases with operation time, while with XPS investigations of active type 2 electrodes no increasing nickel oxide signal is observed for the aged electrodes. The increased part of nickel oxide in the

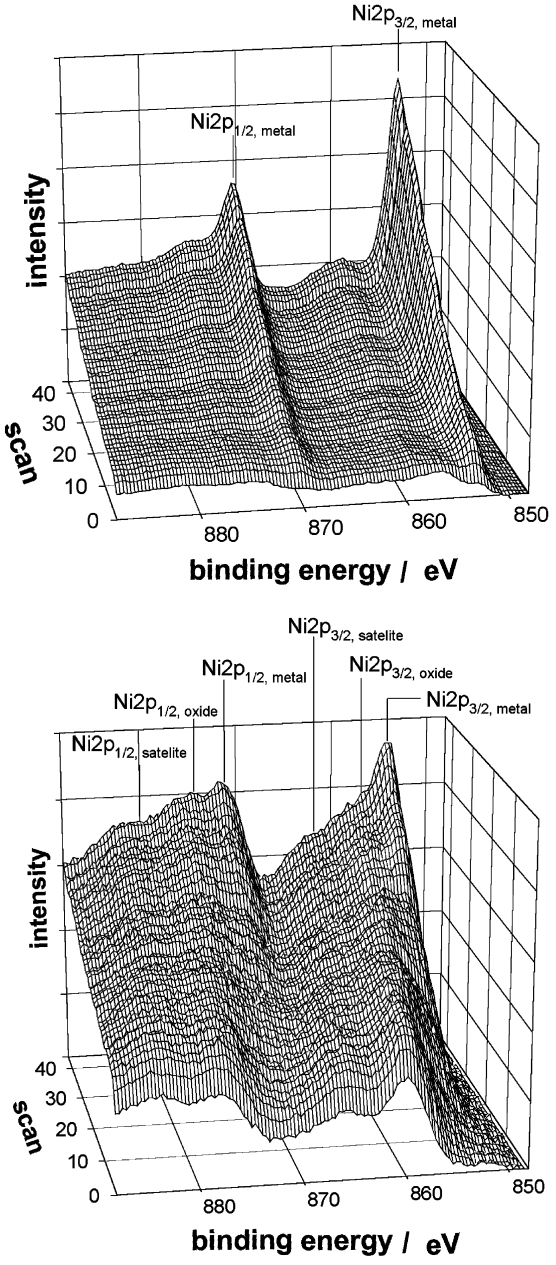

Fig. 6. Ni 2p spectra recorded by X-ray photoelectron spectroscopy of an active (on the top) and an overloaded electrode (on the bottom) of type 3.

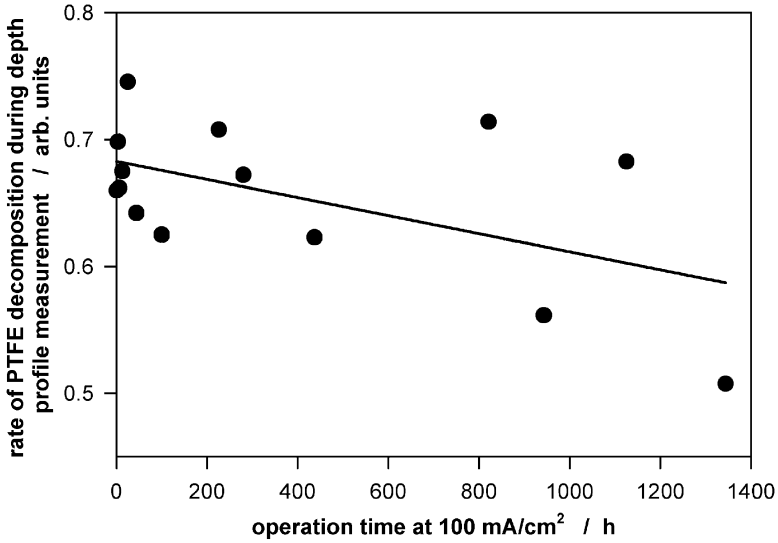

Fig. 7. Decrease of the fluorine concentration during depth profile measurements of type 2 electrodes after different operation times. The solid line is the regression straight line calculated from the data points.

type 3 electrodes may be an artifact of the transfer process from the electrolyte to the analytical methods. The nickel particles can be oxidized on the surface by air or water during the transfer process [68]. The part of the nickel oxide determined by XPS can, thus, depend on the size of the nickel particles and, therefore, the effect would be stronger for the electrodes of type 3 than it would be for electrodes of type 2.

The pore system can also be changed induced by the overloading. For the electrodes of type 2, passivated by overloading the pore frequency is slightly reduced compared with active electrodes with similar operation times, but the difference is not very big. In contrast, for the electrodes of type 3 passivated by overloading the pore frequency is strongly reduced compared with the active electrodes as shown in Fig. 5. Additionally, the specific surface area of the overloaded type 3 electrodes is also reduced.

Due to the differences between the three electrode types, differences in the degradation processes are possible. As there is no copper in the electrodes of type 1 no copper can be solved from these electrodes. The copper in the electrodes of types 2 and 3 is partially solved and the copper distribution in these electrodes is changed as also observed during the activation procedure of type 2 electrodes [45]. The dissolution of the copper is surprising because copper is more noble than the nickel catalyst [69]. Copper, however, is dissolved under basic environmental conditions by a sufficient anodic polarization and in contrast nickel is oxidized, but not dissolved. The changes of the copper distribution in the electrodes show that the electrochemical conditions in the electrodes are locally quite different, and not only locally different but also fluctuant in time.

During long-term operation the polymer in the electrodes is changed caused by the electrochemical stressing [42]. A changed decomposition kinetic of the PTFE induced by ionizing radiation is an observable consequence of the changes of the PTFE induced by the fuel cell operation of the electrodes [42]. These changes are observed for all three electrode types, significant differences between the different electrode types cannot be detected. An indicator for the different rates of PTFE decomposition induced by ionizing radiation is the decrease of the fluorine concentration during XPS depth profile measurements. Fig. 7 shows the decrease of the fluorine concentration recorded for type 2 electrodes after different operation times. The line is a regression straight line calculated for the shown measurement points. The electrochemically induced changes of the PTFE as well as the influence of the operation time can also be deduced from the form of the C 1s spectra during the depth profiles [42].

4. Conclusions

For all the investigated gas diffusion electrodes with nickel catalyst used as anode in AFCs a decrease of the electrochemical performance was observed, which is induced by electrochemical stressing. The decrease of the electrochemical performance is different for the different electrode types; for the electrodes of types 1 and 3 the decrease can be described by an e-function, while for the electrodes of type 2 two e-functions are necessary. For all electrodes a time constant in the e-function of approximately 250 h is observed at a current density of 100 mA/cm^2. This time constant depends on the current density, whereby the dependence on the current density is stronger for the type 3 electrodes than for those of type 2. The second time constant for describing the degradation of the electrochemical performance of type 2 electrodes strongly depends on the current density.

It is surprising that the electrodes with the size selected nickel catalyst nearly have the same time constants as the electrodes with the standard nickel catalyst. The disintegration of the nickel particles, which effect the electrochemical activity, is different. The different time dependences of frequency of pores at 2 nm radius for the electrodes of types 2 and 3 reflect the different nickel particle disintegrations. In contrast to the strong correlation between the electrochemical performance (surface specifical conductivity) and the pore frequency observed for the electrodes of type 2 [61], a strong correlation between these two characteristics could not be observed for the electrodes of type 3. For electrodes of type 3 passivated by overloading the frequency of pores with 2 nm radius is significantly lower than for active electrodes. This effect is significantly lower for type 2 electrodes.

The total passivation of the electrodes is correlated with an oxidation of the nickel catalyst. In the XP spectra of the electrodes passivated by overloading oxidized nickel was observed, as expected. During overloading, the electrode potential becomes so anodic that the nickel is in the oxidation potential. In contrast to the electrodes totally passivated by overloading in the activated by aged type 2 electrodes no significant part of nickel oxide is observed. Therefore, the oxidation of nickel does not generally dominate the degradation process. In the type 3 electrodes, the part of the oxidized nickel increases with operation time and, therefore, the oxidation of the nickel may be relevant for the degradation process of the type 3 electrodes. Thus, it must be expected that the lifetime of the electrodes depends on the current density caused by the higher anodic polarization at higher current density.

In the electrodes of types 2 and 3, the copper distribution changed because the copper is partially dissolved and transported through the surface during operation time, whereby a part of the copper is re-deposited during the transport process. A significant effect for the long-term behavior of the copper cannot be concluded from the measurements shown.

In addition to the decrease of the electrochemical performance and the changes of the metallic parts of the electrodes a change of the PTFE induced by electrochemical stressing is observed. The change of the PTFE leads to an accelerated decomposition kinetic due to ionizing radiation during XPS depth profile measurements. The PTFE is not electrochemically active in the electrode, but it is necessary for the gas transport and the mechanical stability of the electrodes. A change of the transport characteristic could not be observed with the used methods. A change of the mechanical stability can effect the electrical contact between the metallic electrode components and, thus, change the electrical resistance and consequently the active zone of the electrode, but this effect cannot be estimated.

The degradation process seems to be dominated by the disintegration of the nickel particles and by the changes of the PTFE, whereby the contribution of the PTFE changes to the decrease of the electrochemical performance is not quite clear.

The long-term measurements with the nickel AFC anodes show that different degradation processes run in parallel. Comparable changes may also be created in other low temperature fuel cell types, e.g. PEFCs. PTFE is used in these electrodes, too. The changes of the PTFE in PEFC electrodes may influence the transport mechanisms more drastically than in the AFC. By a partial decomposition of the PTFE new chemical groups can be added and so the hydrophobic character can be changed. A change of the PTFE is also observed in PEFC electrodes [33]. The distribution of catalysts in PEFC electrodes is also observed, whereby in contrast to the nickel particles in AFC there is no disintegration observed, but an accumulation [70].

For understanding the degradation process it is not sufficient to study the changes of the electrochemical performance, but the physical characteristics of electrodes must also be investigated.

References

[1] Daimler-Benz HighTech Report, 1997, p. 20.
[2] K. Kordesch, G. Simader, Fuel Cells and Their Applications, VCH Verlag, Weinheim, 1996.
[3] M.S. Wilson, J.A. Valerio, S. Gottesfeld, Electrochim. Acta 40 (1995) 355.
[4] A. Ioselevich, A.A. Kornyshev, W. Lehnert, Solid State Ionics 124 (1999) 221.
[5] A. Ioselevich, A.A. Kornyshev, W. Lehnert, J. Electrochem. Soc. 144 (1997) 3010.
[6] S. Primdahl, M. Mogensen, J. Appl. Electrochem. 30 (2000) 247.
[7] N.M. Sammes, M. Brown, I.W.M. Brown, J. Mater. Sci. 31 (1996) 6069.
[8] S. Wang, Y. Jiang, Y. Zhang, W. Li, J. Yan, Z. Lu, Solid State Ionics 120 (1999) 75.
[9] T. Matsushima, H. Ohrui, T. Hirai, J. Power Sources 71 (1998) 185.
[10] A.L. Dicks, J. Power Sources 71 (1998) 111.
[11] S. Taniguchi, M. kadowaki, H. Kawamura, T. Yasuo, Y. Akiyama, Y. Miyake, T. Saitoh, J. Power Sources 55 (1995) 73.
[12] H.Y. Tu, Y. Takeda, N. Imanishi, O. Yammamoto, Solid State Ionics 117 (1999) 277.
[13] M.B. Phillipps, N.M. Sammes, O. Yammamoto, J. Mater. Sci. 31 (1996) 1689.
[14] H.Y. Tu, Y. Takeda, N. Imanishi, O. Yammamoto, Solid State Ionics 100 (1997) 283.
[15] M. Hrovat, S. Bernik, J. Holc, D. Kolar, B. Dacar, J. Mater. Sci. Lett. 14 (1995) 1684.
[16] S.P.S. Badwal, F.T. Chacchi, S. Rajendran, J. Drennan, Solid State Ionics 109 (1998) 167.
[17] J.H. Choi, J.H. Jang, J.H. Ryu, S.M. Oh, J. Power Sources 87 (2000) 92.
[18] C. Brugnoni, U. Ducati, M. Scagliotti, Solid State Ionics 76 (1995) 177.
[19] M.J. Jorgensen, P. Holtappels, C.C. Appel, J. Appl. Elelctrochem. 30 (2000) 411.
[20] K. Huang, M. Feng, J.B. Goodenough, Solid State Ionics 89 (1996) 17.
[21] S. Zhuiykov, J. Eur. Ceram. Soc. 20 (2000) 967.
[22] S.P.S. Badwal, F.T. Chacchi, S. Rajendran, J. Drennan, Solid State Ionics 109 (1998) 167.
[23] I.R. Gibson, G.P. Dransfield, J.T.S. Irvine, J. Eur. Ceram. Soc. 18 (1998) 661.
[24] W.J. Quadakkers, H. Greiner, M. Hänsel, A. Pattanaik, A.S. Khanna, W. Mallener, Solid State Ionics 91 (1996) 55.
[25] S.P. S Badwal, R. Deller, K. Foger, Y. Ramprakash, J.P. Zhang, Solid State Ionics 99 (1997) 297.

[26] K. Huang, P.Y. Hou, J.B. Goodenough, Solid State Ionics 129 (2000) 237.
[27] D.P. Davies, P.L. Adcock, M. Turpin, S.J. Rowen, J. Appl. Electrochem. 30 (2000) 101.
[28] D.P. Davies, P.L. Adcock, M. Turpin, S.J. Rowen, J. Power Sources 86 (2000) 237.
[29] B. Mattsson, H. Ericson, L.M. Torell, F. Sundfolm, Electrochim. Acta 45 (2000) 1405.
[30] E. Hübner, J. Roduner, Mater. Chem. 9 (1999) 409.
[31] M. Schulze, M. Lorenz, N. Wagner, E. Gülzow, Fresenius J. Anal. Chem. 365 (1999) 106.
[32] F.N. Büchi, B. Gupta, O. Haas, G.G. Scherer, Electrochim. Acta 40 (1995) 345.
[33] E. Gülzow, A. Helmbold, T. Kaz, R. Reißner, M. Schulze, N. Wagner, G. Steinhilber, J. Power Sources 86 (2000) 352.
[34] S. Gupta, D. Tryk, S.K. Zecevic, W. Aldred, D. Guo, R.F. Savinell, J. Appl. Electrochem. 28 (1998) 673.
[35] E. Gülzow, M. Fischer, A. Helmbold, R. Reißner, M. Schulze, N. Wagner, M. Lorenz, B. Müller, T. Kaz, Innovative production technique for PEFC and DMFC electrodes and degradation of MEA-components, in: Proceedings of the Fuel Cell Seminar 16–19 November 1998, Palm Springs, 1998, p. 469.
[36] E. Gülzow, T. Kaz, M. Lorenz, A. Schneider, M. Schulze, Degradation of PEFC components, in: Proceedings of the Fuel Cell Seminar 2000, Portland, 30 October–2 November 2000, p. 156.
[37] M.S. Wilson, J.A. Valerio, S. Gottesfeld, Electrochim. Acta 40 (1995) 355.
[38] P.G. Dirven, W.J. Engelen, C.J.M. Van Der Poorten, J. Appl. Electrochem. 25 (1995) 122.
[39] S. Gultekin, M.A. Al-Saheh, A.S. Al-Zakri, K.A.A. Abbas, Int. J. Hydrogen Energy 21 (1996) 485.
[40] Y. Kiros, S. Schwartz, J. Power Sources 87 (2000) 101.
[41] M.A. Al-Saleh, A.S. Al-Zakri, S. Gultekin, J. Appl. Electrochem. 27 (1997) 215.
[42] M. Schulze, K. Bolwin, E. Gülzow, W. Schnurnberger, Fresenius J. Anal. Chem. 353 (1995) 778.
[43] E. Gülzow, et al., PTFE bonded gas diffusion electrodes for alkaline fuel cells, in: Proceedings of the 9th World Hydrogen Energy Conference, 1992, Paris, p. 1507.
[44] A. Khalidi, B. Lafage, P. Taxil, G. Gave, M.J. Clifton, P. Cezac, Int. J. Hydrogen Energy 21 (1996) 25.
[45] M. Schulze, E. Gülzow, G. Steinhilber, Appl. Surf. Sci. 179 (2001) 252.
[46] N. Wagner, E. Gülzow, M. Schulze, W. Schnurnberger, Gas diffusion electrodes for alkaline fuel cells in solar hydrogen energy, in: H Steeb, H. Aba Oud (Eds.), German–Saudi Joint Program on Solar Hydrogen Production and Utilization Phase II, 1992–1995, Stuttgart 1996, ISBN 3-89100-028-6.
[47] H. Sauer, German Patent DE 2,941,774 (CI H01M4/88).
[48] A. Winsel, German Patent DE 3,342,969 (CI C25B11/06).
[49] E. Gülzow, K. Bolwin, W. Schnurnberger, Dechema-Monographien Bd 117 (1989) 365.
[50] E. Gülzow, W. Schnurnberger, Dechema-Monographien Bd 124 (1991) 675.
[51] E. Gülzow, K. Bolwin, W. Schnurnberger, Dechema-Monographien Bd 121 (1990) 483.
[52] E. Gülzow, K. Bolwin, W. Schnurnberger, Dechema-Monographien Bd 117 (1989) 365.
[53] E. Gülzow, K. Bolwin, W. Schnurnberger, in: H. Wendt, V. Plzak (Eds.), Brennstoffzellen, Hrsg. VDI-Verlag, Düsseldorf, 1990.
[54] E. Gülzow, B. Holzwarth, M. Schulze, N. Wagner, W. Schnurnberger, Dechema Monographien Bd 125 (1992) 561.
[55] M.A. Sleem-Ur-Rahman, A.S. Al-Saleh, S. Al-Zakri, J. Gultekin, Appl. Electrochem. 27 (1997) 215.
[56] E. Gülzow, et al., Fuel Cell Bulletin 15, Dez, 1999, pp. 8–12.
[57] D. Bevers, E. Gülzow, A. Helmbold, B. Müller, Innovative production technique for PEFC electrodes, in: Proceedings of the Fuel Cell Seminar, Orlando, 1996, p. 668.
[58] A. Helmbold, German Patent DE 197,57,492 A1 (1999).
[59] D. Bevers, N. Wagner, German Patent DE 195,09,749 C2.
[60] N. Wagner, German Patent DE 19509748.
[61] M. Schulze, E. Gülzow, G. Steinhilber, in press.
[62] Justi, Winsel, Kalte Verbrennung, Franz Steiner Verlag GmbH, Wiesbaden, 1962, p. 117.
[63] G. Ertl, J. Küppers, Low Energy Electron and Surface Spectroscopy, VCH-Verlagsgesellschaft, Weinheim, 1985.
[64] S.J. Gregg, K.S.W. Sing, Adsorption, Surface Area and Porosity, Academic Press, London, 1982.
[65] Carlo Erba Microstructure Line no. 5, 1987, p. 1.
[66] J.F. Moulder, W.F. Stickle, P.E. Sobol, K.D. Bomben, in: J. Chastain, R.C. King (Eds.), Handbook of X-ray Photoelectron Spectroscopy, Physical Electronics Inc., Minnesota, 1995.
[67] M. Schulze, R. Reißner, M. Lorenz, W. Schnurnberger, Electrochim. Acta 44 (1999) 3969.
[68] M. Lorenz, M. Schulze, Surf. Sci. 454–456 (2000) 234.
[69] M. Pourbaix, Atlas of Electrochemical Equilibria in Aqueous Solutions, Pergamon Press, Oxford, 1966.
[70] A. Schneider, Private communication; M. Schulze, A. Schneider, in preparation.